

Research

Open Access

## A dynamic model of gene expression in monocytes reveals differences in immediate/early response genes between adult and neonatal cells

Shelley Lawrence<sup>†1</sup>, Yuhong Tang<sup>†2</sup>, M Barton Frank<sup>2</sup>, Igor Dozmorov<sup>2</sup>, Kaiyu Jiang<sup>1</sup>, Yanmin Chen<sup>1</sup>, Craig Cadwell<sup>2</sup>, Sean Turner<sup>2</sup>, Michael Centola<sup>2</sup> and James N Jarvis\*<sup>1</sup>

Address: <sup>1</sup>Dept. of Pediatrics, Neonatal Section, University of Oklahoma College of Medicine, Oklahoma City, OK, USA and <sup>2</sup>Arthritis & Immunology Program Oklahoma Medical Research Foundation, Oklahoma City, 73104, USA

Email: Shelley Lawrence - lawrence@pediatrics.com; Yuhong Tang - yuhong-tang@omrf.ouhsc.edu; M Barton Frank - Bart-Frank@omrf.ouhsc.edu; Igor Dozmorov - igor-dozmorov@omrf.ouhsc.edu; Kaiyu Jiang - kaiyu-jiang@ouhsc.edu; Yanmin Chen - yanmin-Chen@ouhsc.edu; Craig Cadwell - craig-cadwell@omrf.ouhsc.edu; Sean Turner - sean-turner@omrf.ouhsc.edu; Michael Centola - michael-centola@omrf.ouhsc.edu; James N Jarvis\* - james-jarvis@ouhsc.edu

\* Corresponding author    †Equal contributors

Published: 16 February 2007

Received: 26 September 2006

Journal of Inflammation 2007, **4**:4 doi:10.1186/1476-9255-4-4

Accepted: 16 February 2007

This article is available from: <http://www.journal-inflammation.com/content/4/1/4>

© 2007 Lawrence et al; licensee BioMed Central Ltd.

This is an Open Access article distributed under the terms of the Creative Commons Attribution License (<http://creativecommons.org/licenses/by/2.0>), which permits unrestricted use, distribution, and reproduction in any medium, provided the original work is properly cited.

### Abstract

Neonatal monocytes display immaturity of numerous functions compared with adult cells. Gene expression arrays provide a promising tool for elucidating mechanisms underlying neonatal immune function. We used a well-established microarray to analyze differences between LPS-stimulated human cord blood and adult monocytes to create dynamic models for interactions to elucidate observed deficiencies in neonatal immune responses.

We identified 168 genes that were differentially expressed between adult and cord monocytes after 45 min incubation with LPS. Of these genes, 95% (159 of 167) were over-expressed in adult relative to cord monocytes. Differentially expressed genes could be sorted into nine groups according to their kinetics of activation. Functional modelling suggested differences between adult and cord blood in the regulation of apoptosis, a finding confirmed using annexin binding assays. We conclude that kinetic studies of gene expression reveal potentially important differences in gene expression dynamics that may provide insight into neonatal innate immunity.

### Background

The defects in neonatal adaptive immunity are relatively easy to understand *a priori*. Although there are complexities to be considered [1,2], experimental evidence demonstrates that newborns, lacking prior antigen exposure, must develop immunologic memory based on postnatal experience with pathogens and environmental immunogens [3-5].

It is less clear why there should be defects in newborns' innate immunity, although these defects are well documented. For example, newborns have long been known to exhibit defects in phagocytosis [6], chemotaxis [7,8], and adherence [9], the latter possibly due to aberrant regulation of critical cell-surface proteins that mediate leukocyte-endothelial interactions [10]. Newborn monocytes

also exhibit diminished secretion of numerous cytokines under both stimulated and basal conditions [11-13].

Elucidating the causes of these defects is a crucial question in neonatal medicine, since infection remains a major cause of morbidity and mortality in the newborn period. However, unravelling the complex events in monocyte and/or neutrophil activation, from ligand binding to activation of effector responses, is clearly a daunting challenge. Any one of numerous pathways from the earliest cell signalling events to protein synthesis or secretion could be relevant, and focusing on any one may overlook critical aspects of cellular regulation. In this context, genomic and/or proteomic approaches may offer some important advantages, at least in the initial phases of investigation, by allowing investigators to survey the panoply of biological processes that may be relevant to identifying critical biological distinctions.

Recently published work has documented differences in gene expression between adult and cord blood monocytes [14], although these studies did not elucidate the fundamental, functional differences between cord blood and adult cells. The studies we report here demonstrate how computational analyses, applied to microarray data, can elucidate critical biological functions when analysis extends beyond the identification of differentially-expressed genes.

## Methods

### **Cells and cellular stimulation**

Monocytes were purified from cord blood of healthy, term infants and from the peripheral blood of healthy adults by positive selection using anti-CD-14 mAb-coated magnetic beads (Miltenyi Biotec, Auburn, CA, USA) according to the manufacturer's instructions. Informed consent was obtained from adult volunteers; collection of cord blood was ruled exempt from consent after review by the Oklahoma Health Sciences Center IRB. In brief, blood was collected into sterile tubes containing sodium citrate as an anticoagulant (Becton Dickinson, Franklin Lakes, NJ). Peripheral blood mononuclear cells (PBMC) were prepared from the anti-coagulated blood using gradient separation on Histopaque-1077 performed directly in the blood collection tubes. Cells were washed three times in  $\text{Ca}^{2+}$  and  $\text{Mg}^{2+}$ -free Hanks's balanced salt solution. PBMC were incubated for 20 min at 4°C with CD14 microbeads at 20  $\mu\text{l}/1 \times 10^7$  cells. The cells were washed once, re-suspended in 500  $\mu\text{l}$   $\text{Ca}^{2+}$  and  $\text{Mg}^{2+}$ -free PBS containing 5% FBS/1  $\times 10^8$  cells. The suspension was then applied to a MACs column. After unlabeled cells passed through, the column was washed with 3  $\times$  500  $\mu\text{l}$   $\text{Ca}^{2+}$  and  $\text{Mg}^{2+}$ -free PBS. The column was removed from the separator and was put on a new collection tube. One ml of  $\text{Ca}^{2+}$  and  $\text{Mg}^{2+}$ -free PBS was then added onto the column, which

was immediately flushed by firmly applying the plunger supplied with the column.

Purified monocytes were incubated with LPS from *Escherichia coli* 0111:4B (Sigma, St. Louis, MO) at 10 ng/ml for 45 min and 2-hours in RPMI 1640 with 10% fetal bovine serum or studied in the absence of stimulation ("zero time"). It should be noted that this product is not "pure," and stimulates both TLR-4 and TRL-2 signaling pathways [15]. A smaller number of replicates ( $n = 5$ ) was analyzed after 24 hr incubation. After the relevant time points, monocytes were lysed with TriZol (Invitrogen, Carlsbad, CA, USA) and RNA was isolated as recommended by the manufacturer. Cells from eight different term neonates and eight different healthy adults were used for these studies.

### **Gene microarrays**

The microarrays used in these experiments were developed at the Oklahoma Medical Research Foundation Microarray Research Facility and contained probes for 21,329 human genes. Slides were produced using commercially available libraries of 70 nucleotide long DNA molecules whose length and sequence specificity were optimized to reduce the cross-hybridization problems encountered with cDNA-based microarrays (Qiagen-Operon). The oligonucleotides were derived from the UniGene and RefSeq databases. The RefSeq database is an effort by the NCBI to create a true reference database of genomic information for all genes of known function. All 11,000 human genes of known or suspected function were represented on these arrays. In addition, most undefined open reading frames were represented (approximately 10,000 additional genes).

Oligonucleotides were spotted onto Corning® Ultra-GAPS™ amino-silane coated slides, rehydrated with water vapor, snap dried at 90°C, and then covalently fixed to the surface of the glass using 300 mJ, 254 nm wavelength ultraviolet radiation. Unbound free amines on the glass surface were blocked for 15 min with moderate agitation in a 143 mM solution of succinic anhydride dissolved in 1-methyl-2-pyrrolidinone, 20 mM sodium borate, pH 8.0. Slides were rinsed for 2 min in distilled water, immersed for 1 min in 95% ethanol, and dried with a stream of nitrogen gas.

### **Labeling, hybridization, and scanning**

Fluorescently labeled cDNA was separately synthesized from 2.0  $\mu\text{g}$  of total RNA using an oligo dT<sub>12-18</sub> primer, PowerScript reverse transcriptase (Clontech, Palo Alto, CA), and Cy3-dUTP (Amersham Biosciences, Piscataway, NJ) for 1 hour at 42°C in a volume of 40  $\mu\text{l}$ . Reactions were quenched with 0.5 M EDTA and the RNA was hydrolyzed by addition of 1 M NaOH for 1 hr at 65°C. The reac-

tion was neutralized with 1 M Tris, pH 8.0, and cDNA was then purified with the Montage PCR<sub>96</sub> Cleanup Kit (Millipore, Billerica, MA). cDNA was added to ChipHybe™ hybridization buffer (Ventana Medical Systems, Tucson, AZ) containing Cot-1 DNA (0.5 mg/ml final concentration), yeast tRNA (0.2 mg/ml), and poly(dA)<sub>40-60</sub> (0.4 mg/ml). Hybridization was performed on a Ventana Discovery system for 6 hr at 42 °C. Microarrays were washed to a final stringency of 0.1× SSC, and then scanned using a dual-color laser (Agilent Biotechnologies, Palo Alto, CA). Fluorescent intensity was measured by Imagene™ software (BioDiscovery, El Segundo, CA).

#### **PCR validation of array data**

##### *Reverse transcription*

Three cord blood samples (C1, C2, and C5) and three adult samples (A1, A5, and A6) from the 45 minute time point were used for PCR validation. First strand cDNA was generated from 3.6 µg of total RNA per sample using the OmniScript Reverse Transcriptase and buffer (Qiagen, Valencia, CA), 1 µl of 100 µM oligo dT primer (dT<sub>15</sub>) in a 40 µl volume. Reactions were incubated 60 min at 37° and inactivated at 93° for 5 min. cDNA was diluted 1:100 in water and stored at -20°C.

##### **Quantitative PCR**

Gene-specific primers for 10 genes (*Erbb3*, *Tmod*, *Dscr1l1*, *Sp1*, *Scya4*, *Gro2*, *Cri1*, *Scya3*, *Scya3l1*, and *Il-1a*) were designed with a 60°C melting temperature and a length of 19–25 bp for PCR products with a length of 90–140 bp, using Applied Biosystems Inc (ABI, Foster City, CA) Primer Express 1.5 software. PCR was run with 2 µl cDNA template in 15 µl reactions in triplicate on an ABI SDS 7700 using the ABI SYBR Green I Master Mix and gene specific primers at a concentration of 1 µM each. The temperature profile consisted of an initial 95°C step for 10 minutes (for Taq activation), followed by 40 cycles of 95°C for 15 sec, 60°C for 1 min, and then a final melting curve analysis with a ramp from 60°C to 95°C over 20 min. Gene-specific amplification was confirmed by a single peak in the ABI Dissociation Curve software. No template controls were run for each primer pair. Since equal amounts of total RNA were used for cDNA synthesis, Ct values should reflect relative abundance [16]. These values were used to calculate the average group Ct (Cord vs. Adult) and the relative ΔCt was used to calculate fold change between the two groups [17].

#### **Apoptosis assays**

Exposed membrane phospholipids (a marker for early apoptosis) were detected in adult and neonatal monocytes after LPS stimulation using a commercially available annexin V binding assay. Monocytes from cord blood and adult peripheral blood were obtained as outlined above. Isolated monocytes were either labeled immediately with

annexin V-FITC or were stimulated for 14 hours with LPS 10 ng/ml prior to labeling (this time point was derived empirically to maximize apoptosis). Annexin V-FITC staining was completed via the Annexin V-FITC Apoptosis Detection Kit I (BD Biosciences, San Jose, CA) using 5 µl of propidium iodine and 5 µl annexin V-FITC as recommended by the manufacturer. Analysis by flow cytometry was accomplished on a FACS Calibur automated bench-top flow cytometer. Data obtained by flow cytometry was analyzed by non-parametric t-test (Mann-Whitney test). An alpha level of 0.05 was considered statistically significant.

#### **Statistical analysis**

Microarrays were normalized and tested for differential expression using methods described previously [18]. Differential expression was concluded if the genes met the following criteria: a minimum expression level at least 10 times above background at one or more time points, a minimum 1.5-fold difference in the mean expression values between groups at one or more time points, and a minimum of 80% reproducibility using the jack-knife method. A jack-knife is the most common type of Leave-one-out-cross-validation (LOOCV); it is used here to cross-validate genes selected by differential analysis [19]. Time series analysis was performed using the hypervariable (HV) gene method previously described by our group [20].

After selection, HV genes are clustered and interrogated for gene-gene interactions. K-means clustering, an unsupervised technique, was performed on the HV genes to create unbiased clusters. Discriminate function analysis (DFA), a supervised technique, was used to determine and spatially map gene-to-gene interactions [21].

All statistical analysis was performed in Matlab R14 (Natick, MA) and Statistica v7 (Tulsa, OK, USA). An alpha level of 0.05 was considered statistically significant for all analyses.

Analysis of the apoptosis assays was undertaken using both parametric and non-parametric analysis methods. Parametric analysis was undertaken using the student's t-test; non-parametric analysis used the Mann-Whitney U-test. A p-value of > 0.05 was the threshold for rejecting the null hypothesis.

#### **Discriminant function analysis**

DFA is a method that identifies a subset of genes whose expression values can be linearly combined in an equation, denoted a root, whose overall value is distinct for a given characterized group. DFA therefore, allows the genes that maximally discriminate among the distinct groups analyzed to be identified. In the present work, a

variant of the classical DFA, named the Forward Stepwise Analysis, was used to select the set of genes whose expression maximally discriminated among experimentally distinct groups. The Forward Stepwise Analysis was built systematically in an iterative manner. Specifically, at each step all variables were reviewed to identify the one that most contributes to the discrimination between groups. This variable was included in the model, and the process proceeded to the next iteration. The statistical significance of discriminative power of each gene was also characterized by partial Wilk's Lambda coefficients, which are equivalent to the partial correlation coefficient generated by multiple regression analyses. The Wilk's Lambda coefficient used a ratio of within-group differences and the sum of within-plus between-group differences. Its value ranged from 1.0 (no discriminatory power) to 0.0 (perfect discriminatory power).

#### *Computer analysis of functional associations between differentially expressed genes*

In addition to the above analyses, genes showing the most significant differences between neonatal and adult cells were characterized functionally using pre-existing databases such as PubMed, BIND, KEGG, and Ontoexpress. Biological associations of the differentially expressed genes were modelled using Ingenuity Pathways Analysis (Redwood City, CA). Data analyzed through this technique can then be resolved into cogent models of the specific biological pathways activated under the experimental conditions used in the microarray analyses.

## Results

### **Differential gene expression analysis**

Table 1 lists genes determined to be differentially expressed between cord and adult peripheral blood monocytes, as described above. No genes were found to be statistically significantly differentially expressed between adult and cord monocytes in the absence of LPS exposure. 168 genes were differentially expressed between adult and cord monocytes after 45 min incubation with LPS. 95% of these genes (159 of 168) were over-expressed in adult relative to cord monocytes. After 120 minutes of LPS exposure, 24 genes were differentially expressed between adult and cord monocytes. Of the latter genes, 23 were more highly expressed in cord than adult monocytes. This pattern of differentially expressed genes suggested an initial delayed response to LPS followed by an enhanced transcription of genes in cord relative to adult monocytes. To test this hypothesis, k-means clustering was used to categorize differentially expressed genes based on their temporal profiles. Relative decreases in gene transcription by cord monocytes at 45 min were seen in 6 of the 9 clusters (Figure 1). Each of these clusters contained between 15 and 46 genes. Examination of the clusters showed that differences between groups after 45 minutes of LPS exposure

were attributable to a) genes in certain clusters that were up-regulated in adult monocytes only, b) genes in other clusters that were down-regulated in cord monocytes only, or c) genes in yet other clusters that were up-regulated in adult and down-regulated in cord monocytes. These results, summarized in a heat map in Figure 2, indicated a high complexity of gene expression differences between adult monocytes and cord blood monocytes in response to LPS.

In addition to the above genes which differed in expression between groups following LPS exposure, 516 genes were also identified that were differentially expressed over time within a group. A supplementary table containing these data is available upon request. For these genes, a similar pattern of dynamic expression was seen as was observed in the other group. Therefore, these genes reflect common responses to LPS in monocytes from both sources.

A subset of genes that were differentially expressed either between adult and cord blood monocytes were selected for validation using the quantitative real-time polymerase chain reaction method (QRT-PCR). These included four genes that differed between groups after 45 min of LPS exposure (*Erbb3*, *Tmod*, *Dscr1l1*, and *Sp1*), and six genes that differed in expression after 2 hours of LPS exposure (*Scya4*, *Gro2*, *Cri1*, *Scya3*, *Scya3l1*, and *Il-1a*). Nine of the ten genes tested for QRT-PCR validation demonstrated similar levels of relative expression in QRT-PCR experiments as in the microarrays. Only *CRI1* failed to corroborate the microarray data.

### **Hypervariable gene analysis**

One hundred eighty-eight hypervariable (HV) genes were selected from expressed genes in adult and cord blood monocytes based on their changes across three time points. These genes exhibited significantly higher expression variation over time than the majority of genes. Differences in variation between two experimental sample sets, in this case adult and neonatal samples, can represent differences in homeostatic control mechanisms between these two sets [20]. The selected genes were hypervariable in both sample groups. HV genes with highly correlated expression levels in a given population are likely to share function [20]. A correlation based clustering procedure was carried out for these HV genes as described in the methods section. Genes belonging to the 5 largest clusters were used for creation of a graphical output, denoted a correlation mosaic. A correlation mosaic allows identification of the genes within clusters by visual inspection and subsequent functional analysis of genes within clusters (Figures 3A &3B). Figure 3A represents 110 genes of the same cluster allocation between adult and cord blood monocyte samples, demonstrating a very high similarity

**Table I: Differentially expressed genes between adult and cord monocytes at specific time points. T = time (min) at which the sample was taken. Numbers indicate corrected expression values.**

	Genbank #	Symbol	Gene Description	Adult	Adult	Adult	Cord	Cord	
				T = 0	t = 45	t = 120	t = 0	t = 45	t = 120
<b>Apoptosis</b>									
	<u>NM_033423</u>	CTLA1	Similar to granzyme B (granzyme 2, cytotoxic T-lymphocyte-associated serine esterase 1)	317	<b>419</b>	299	199	<b>193</b>	264
	<u>AB037796</u>	PDCD6IP	Programmed cell death 6 interacting protein	75	<b>155</b>	68	79	<b>70</b>	81
	<u>NM_024969</u>	TAIP-2	TGFb-induced apoptosis protein 2	63	<b>113</b>	107	53	<b>68</b>	116
	<u>NM_003127</u>	SPTAN1	Spectrin, alpha, non-erythrocytic 1 (alpha-fodrin)	713	842	<b>1171</b>	724	824	<b>2093</b>
<b>Protein synthesis, processing, degradation</b>									
	<u>AK001313</u>	RPLP0	Ribosomal protein, large, P0	704	<b>1465</b>	947	703	<b>756</b>	669
	<u>NM_006799</u>	PRSS21	Protease, serine, 21 (testisin)	204	<b>789</b>	457	169	<b>360</b>	400
	<u>NM_003774</u>	GALNT4	UDP-N-acetyl-alpha-D-galactosamine:polypeptide N-acetylgalactosaminyltransferase 4 (GalNAc-T4)	576	<b>651</b>	648	528	<b>378</b>	578
	<u>AK057790</u>		cDNA FLJ25061 fis, clone CBL04730	245	<b>373</b>	302	244	<b>215</b>	200
	<u>NM_004223</u>	UBE2L6	Ubiquitin-conjugating enzyme E2L 6	128	<b>191</b>	146	108	<b>99</b>	109
	<u>NM_014710</u>	GPRASPI	KIAA0443 gene product	122	<b>182</b>	106	113	<b>119</b>	95
	<u>NM_021090</u>	MTMR3	Myotubularin related protein 3	109	<b>171</b>	137	108	<b>87</b>	138
	<u>AF339824</u>	HS6ST3	Heparan sulfate 6-O-sulfotransferase 3	89	<b>112</b>	91	94	<b>46</b>	76
	<u>NM_012180</u>	FBXO8	F-box only protein 8	40	<b>67</b>	42	45	<b>33</b>	43
	<u>U66589</u>	RPL5	Ribosomal protein L5	34	<b>48</b>	37	30	<b>26</b>	36
	<u>NM_001870</u>	CPA3	Carboxypeptidase A3 (mast cell)	183	<b>495</b>	610	146	<b>949</b>	756
	<u>NM_006145</u>	DNAJBI	Dnaj (Hsp40) homolog, subfamily B, member 1	179	277	<b>408</b>	168	299	<b>745</b>
	<u>AK025547</u>	MRPL30	Mitochondrial ribosomal protein L30	83	<b>118</b>	<b>126</b>	81	101	<b>211</b>
	<u>NM_000439</u>	PCSK1	Proprotein convertase subtilisin/kexin type 1	39	55	<b>53</b>	40	78	<b>88</b>
<b>Cell/Organism Movement</b>									
	<u>NM_002067</u>	GNA11	Guanine nucleotide binding protein (G protein), alpha 11 (Gq class)	555	<b>870</b>	607	540	<b>468</b>	664
	<u>NM_002465</u>	MYBPC1	Myosin binding protein C, slow type	81	<b>140</b>	154	88	<b>80</b>	161
	<u>NM_003275</u>	TMOD	Tropomodulin	276	<b>151</b>	481	257	<b>344</b>	503
	<u>AK026164</u>	MYL6	Myosin, light polypeptide 6, alkali, smooth muscle and non-muscle	7	<b>6</b>	48	5	<b>16</b>	11
<b>Small Molecule Interactions</b>									
	<u>NM_006030</u>	CACNA2D2	Calcium channel, voltage-dependent, alpha 2/delta subunit 2	670	<b>1390</b>	1021	641	<b>639</b>	946
	<u>AK025170</u>	SFXN5	FLJ21517 fis, clone COL05829	431	<b>537</b>	437	405	<b>295</b>	374
	<u>NM_021097</u>	SLC8A1	Solute carrier family 8 (sodium/calcium exchanger), member 1	396	<b>456</b>	458	412	<b>276</b>	369
<b>Signal Transduction</b>									
	<u>NM_032144</u>	RAB6C	RAB6C	827	<b>1658</b>	1307	626	<b>773</b>	1251
	<u>NM_001982</u>	ERBB3	V-erb-b2 erythroblastic leukemia viral oncogene homolog 3	603	<b>1375</b>	671	555	<b>584</b>	643
	<u>AK026479</u>	SNX14	Sorting nexin 14	682	<b>1207</b>	879	624	<b>567</b>	883
	<u>NM_018979</u>	PRKWN K1	Protein kinase, lysine deficient 1	451	<b>813</b>	782	516	<b>480</b>	792
	<u>NM_004811</u>	LPXN	Leupaxin	329	<b>539</b>	445	323	<b>298</b>	503
	<u>BC005365</u>		clone IMAGE:3829438, mRNA, partial cds	257	<b>418</b>	275	275	<b>275</b>	206
	<u>NM_004723</u>	ARHGEF2	Rho/rac guanine nucleotide exchange factor (GEF) 2	215	<b>300</b>	228	197	<b>176</b>	186
	<u>AF130093</u>	MAP3K4	Mitogen-activated protein kinase kinase kinase 4	237	<b>285</b>	275	221	<b>171</b>	223
	<u>AK000383</u>	MKPX	Mitogen-activated protein kinase phosphatase x	218	<b>221</b>	244	233	<b>126</b>	197
	<u>NM_022304</u>	HRH2	Histamine receptor H2	45	<b>121</b>	86	42	<b>74</b>	79
	<u>NM_030753</u>	WNT3	Wingless-type MMTV integration site family member 3	105	<b>117</b>	92	109	<b>63</b>	81
	<u>AB024574</u>	GTPBP2	GTP binding protein 2	89	<b>90</b>	99	74	<b>57</b>	92
	<u>NM_002836</u>	PTPRA	Protein tyrosine phosphatase, receptor type, A	8	<b>6</b>	80	6	<b>16</b>	28
	<u>NM_003656</u>	CAMK1	Calcium/calmodulin-dependent protein kinase I	4940	10131	<b>4446</b>	4785	4907	<b>7190</b>
<b>Cellular Metabolism &amp; Cell Division</b>									
	<u>NM_006170</u>	NOL1	Nucleolar protein 1 (120 kD)	575	<b>1815</b>	1021	499	<b>896</b>	1093

**Table I: Differentially expressed genes between adult and cord monocytes at specific time points. T = time (min) at which the sample was taken. Numbers indicate corrected expression values. (Continued)**

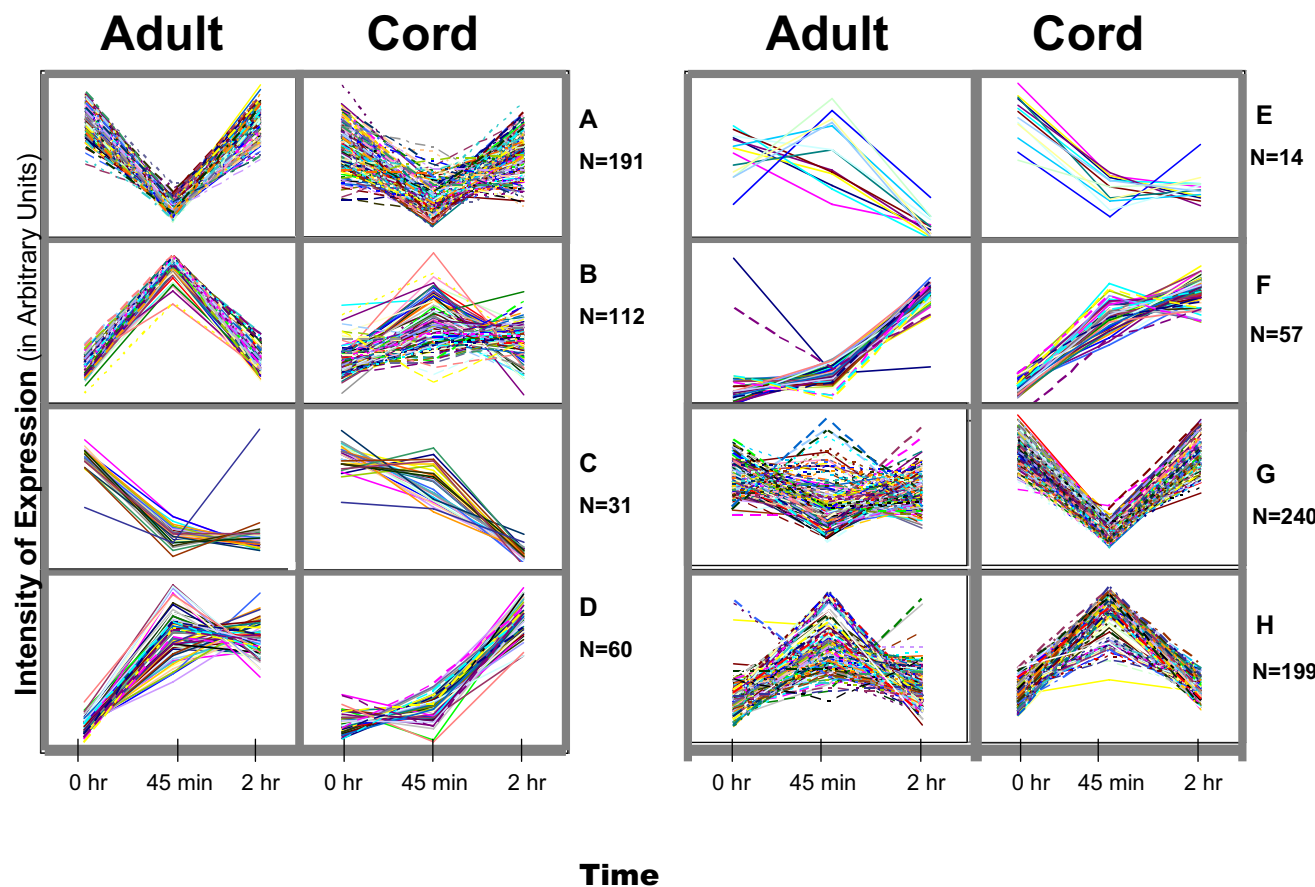
<u>AL133115</u>	COVAI	Cytosolic ovarian carcinoma antigen I	1381	<b>1294</b>	848	1309	<b>658</b>	808
<u>D86962</u>	GRB10	Growth factor receptor-bound protein 10	619	<b>906</b>	200	609	<b>512</b>	179
<u>NM_005628</u>	SLC1A5	Solute carrier family 1 (neutral amino acid transporter), member 5	338	<b>801</b>	600	311	<b>397</b>	524
<u>D17525</u>	MASPI	Mannan-binding lectin serine protease 1 (C4/C2 activating component of Ra-reactive factor)	372	<b>654</b>	43	361	<b>325</b>	55
<u>NM_016518</u>	PIPOX	Pipecolic acid oxidase	240	<b>545</b>	330	221	<b>293</b>	286
<u>NM_012157</u>	FBXL2	F-box and leucine-rich repeat protein 2	274	<b>501</b>	374	249	<b>277</b>	298
<u>NM_018446</u>	AD-017	Glycosyltransferase AD-017	301	<b>369</b>	337	288	<b>223</b>	327
<u>NM_001609</u>	ACADS	Acyl-Coenzyme A dehydrogenase, short/branched chain	354	<b>368</b>	325	273	<b>211</b>	276
<u>NM_001647</u>	APOD	Apolipoprotein D	259	<b>358</b>	289	261	<b>202</b>	205
<u>NM_012113</u>	CA14	Carbonic anhydrase XIV	218	<b>356</b>	279	251	<b>194</b>	270
<u>AB067472</u>	DKFZP4 34L1435	KIAA1885 protein	150	<b>213</b>	186	166	<b>119</b>	163
<u>NM_002916</u>	RFC4	Replication factor C (activator 1) 4 (37 kD)	102	<b>177</b>	119	105	<b>86</b>	132
<u>NM_004889</u>	ATP5j2	ATP synthase, H <sup>+</sup> transporting, mitochondrial F0 complex, subunit f, isoform 2	106	<b>147</b>	76	102	<b>76</b>	62
<u>AK057066</u>		cDNA FLJ32504 fis, clone SMINT1000016, weakly similar to 2-hydroxyacyl sphingosine 1b	69	<b>121</b>	126	64	<b>75</b>	84
<u>AK021722</u>	AGPAT5	Lysophosphatidic acid acyltransferase, epsilon	37	<b>71</b>	48	42	<b>39</b>	46
<u>NM_003664</u>	AP3B1	Adaptor-related protein complex 3, beta 1 subunit	34	<b>52</b>	29	37	<b>24</b>	30
<u>AF146760</u>	Sept10	Septin 10	22	<b>36</b>	23	26	<b>16</b>	28
<u>NM_004910</u>	PITPNM	Phosphatidylinositol transfer protein, membrane-associated	2611	<b>2809</b>	2410	2974	<b>4590</b>	2675
<u>NM_018216</u>	FLJ10782	Pantothenic acid kinase	10	<b>9</b>	10	9	<b>18</b>	15
<u>NM_001714</u>	BICD1	Bicaudal D homolog 1 (Drosophila)	230	562	<b>407</b>	197	447	<b>691</b>
<u>AK054944</u>	LENG5	Leukocyte receptor cluster (LRC) member 5	67	100	<b>91</b>	78	74	<b>158</b>
<b>Gene Expression</b>								
<u>NM_005088</u>	DXYS15 5E	DNA segment on chromosome X and Y (unique) 155 expressed sequence	4857	<b>3489</b>	3214	5177	<b>2241</b>	2725
<u>NM_006298</u>	ZNF192	Zinc finger protein 192	552	<b>988</b>	761	537	<b>578</b>	820
<u>NM_004991</u>	MDS1	Myelodysplasia syndrome 1	401	<b>691</b>	480	390	<b>361</b>	420
<u>NM_021784</u>	HNF3B	Hepatocyte nuclear factor 3, beta	320	<b>632</b>	367	347	<b>361</b>	391
<u>AF153201</u>	LOC585 02	C2H2 (Kruppel-type) zinc finger protein	288	<b>532</b>	335	244	<b>297</b>	324
<u>NM_025212</u>	IDAX	Dvl-binding protein IDAX (inhibition of the Dvl and Axin complex)	297	<b>490</b>	311	303	<b>254</b>	241
<u>AK022962</u>	PBX1	Pre-B-cell leukemia transcription factor 1	237	<b>456</b>	326	245	<b>261</b>	345
<u>NM_017617</u>	NOTCH 1	Notch-1 homolog	309	<b>358</b>	353	324	<b>208</b>	370
<u>NM_001451</u>	FOXF1	Forkhead box F1	165	<b>347</b>	306	177	<b>208</b>	328
<u>NM_007136</u>	ZNF80	Zinc finger protein 80 (pT17)	199	<b>269</b>	203	205	<b>143</b>	177
<u>NM_021975</u>	RELA	V-rel reticuloendotheliosis viral oncogene homolog A, nuclear factor of kappa light polypeptide gene	184	<b>221</b>	139	150	<b>124</b>	122
<u>NM_031214</u>	TARDBP	TAR DNA binding protein	76	<b>154</b>	109	74	<b>91</b>	90
<u>NM_014007</u>	ZNF297B	Zinc finger protein 297B	109	<b>137</b>	122	109	<b>77</b>	111
<u>NM_014938</u>	MONDO A	Mlx interactor	74	<b>90</b>	92	69	<b>53</b>	86
<u>NM_005822</u>	DSCR1L I	Down syndrome critical region gene 1-like 1	45	<b>80</b>	30	40	<b>27</b>	26
<u>NM_004289</u>	NFE2L3	Nuclear factor (erythroid-derived 2)-like 3	73	<b>63</b>	41	64	<b>39</b>	38
<u>NM_054023</u>	SCGB3A 2	Secretoglobin family 3a, member 2	37	<b>59</b>	45	43	<b>34</b>	49
<u>NM_012107</u>	BP75	Bromodomain containing protein 75 kDa human homolog	44	<b>51</b>	34	37	<b>22</b>	30
<u>NM_007212</u>	RNF2	Ring finger protein 2	48	<b>40</b>	30	45	<b>18</b>	26
<u>D89859</u>	ZFP161	Zinc finger protein 161 homolog (mouse)	500	596	<b>4280</b>	458	481	<b>6699</b>
<u>NM_014335</u>	CRII	CREBBP/EP300 inhibitory protein 1	52	84	<b>86</b>	57	72	<b>196</b>
<b>Immune Function</b>								
<u>NM_014889</u>	MPI	Metalloprotease 1 (pitrilysin family)	352	<b>401</b>	398	379	<b>260</b>	351
<u>NM_014312</u>	CTXL	Cortical thymocyte receptor (X. laevis CTX) like	386	<b>370</b>	375	392	<b>224</b>	299
<u>NM_002053</u>	GBPI	Guanylate binding protein 1, interferon-inducible, 67 kD	259	<b>369</b>	334	245	<b>214</b>	251
<u>NM_005356</u>	LCK	Lymphocyte-specific protein tyrosine kinase	186	<b>206</b>	187	235	<b>124</b>	181
<u>NM_000564</u>	IL5RA	Interleukin 5 receptor, alpha	112	<b>106</b>	124	121	<b>63</b>	150
<u>NM_001311</u>	CRIP1	Cysteine-rich protein 1 (intestinal)	45	<b>31</b>	39	49	<b>60</b>	43

**Table I: Differentially expressed genes between adult and cord monocytes at specific time points. T = time (min) at which the sample was taken. Numbers indicate corrected expression values. (Continued)**

<b>Miscellaneous Functions</b>	<u>NM_002984</u>	SCYA4	Small inducible cytokine A4 MIP1B	492	2001	<b>2483</b>	517	1523	<b>3897</b>
	<u>NM_002983</u>	SCYA3	Small inducible cytokine A3 MIP1A	248	1798	<b>2207</b>	185	1364	<b>3673</b>
	<u>NM_014443</u>	IL17B	Interleukin 17B	663	696	<b>681</b>	706	703	<b>1155</b>
	<u>NM_006018</u>	HM74	Putative chemokine receptor-GTP-binding protein	13	25	<b>19</b>	15	26	<b>34</b>
	<u>AB033041</u>	VANGL2	Vang, van gogh-like 2 (Drosophila)	983	<b>1246</b>	1351	981	<b>796</b>	1304
<b>Unknown Function</b>	<u>AK021444</u>	POSTN	Periostin, osteoblast specific factor	569	<b>917</b>	789	522	<b>479</b>	629
	<u>NM_003691</u>	STK16	Serine/threonine kinase 16	403	<b>777</b>	458	395	<b>348</b>	393
	<u>NM_006438</u>	COLECI0	Collectin sub-family member 10 (C-type lectin)	284	<b>762</b>	500	260	<b>351</b>	528
	<u>AK057699</u>		FLJ33137 fis, clone UTERU1000077	375	<b>637</b>	613	369	<b>392</b>	616
	<u>NM_017671</u>	C20orf42	Chromosome 20 open reading frame 42	362	<b>557</b>	551	280	<b>323</b>	478
	<u>AK054683</u>	DCLRE1C	DNA cross-link repair 1C	486	<b>555</b>	574	476	<b>293</b>	515
	<u>NM_033060</u>	KAP4.10	Keratin associated protein 4.10	210	<b>245</b>	197	154	<b>123</b>	172
	<u>AF319045</u>	CNTNAP2	Contactin associated protein-like 2	112	<b>215</b>	173	120	<b>113</b>	176
	<u>NM_001046</u>	SLC12A2	Solute carrier family 12 (sodium/potassium/chloride transporters), member 2	158	<b>148</b>	184	146	<b>86</b>	161
	<u>NM_016279</u>	CDH9	Cadherin 9, type 2 (T1-cadherin)	77	<b>112</b>	69	65	<b>51</b>	64
	<u>NM_014208</u>	DSPP	Dentin sialophosphoprotein	60	<b>90</b>	64	57	<b>53</b>	59
	<u>NM_015669</u>	PCDHB5	Protocadherin beta 5	92	<b>83</b>	62	98	<b>42</b>	47
	<u>AK023198</u>	OPRK1	Opioid receptor, kappa 1	58	<b>76</b>	41	48	<b>46</b>	38
	<u>NM_018240</u>	KIRREL	Kin of IRRE like (Drosophila)	60	<b>75</b>	47	66	<b>43</b>	46
	<u>AK056781</u>	ROCK1	Rho-associated, coiled-coil containing protein kinase 1	54	<b>62</b>	42	47	<b>41</b>	42
	<u>NM_022123</u>	NPAS3	Basic-helix-loop-helix-PAS protein	17	<b>22</b>	9	16	<b>12</b>	13
	<u>NM_001246</u>	ENTPD2	Ectonucleoside triphosphate diphosphohydrolase 2	3438	3272	<b>3731</b>	3767	3590	<b>6309</b>
<b>Unknown Function</b>	<u>AK056884</u>		FLJ32322 fis, clone PROST2003577	2007	<b>2878</b>	2008	1825	<b>1548</b>	1958
	<u>NM_017812</u>	FLJ20420	Coiled-coil-helix-coiled-coil-helix domain containing 3	1105	<b>1915</b>	1370	1125	<b>940</b>	1358
	<u>AJ420459</u>	LOC51184	Protein x 0004	661	<b>1579</b>	881	603	<b>771</b>	768
	<u>BC011575</u>		Similar to RIKEN cDNA 0610031j06 gene, clone IMAGE:4639306	974	<b>1556</b>	1412	1020	<b>844</b>	1261
	<u>AK057357</u>	FLJ32926	DKFZp434D2472	1188	<b>1378</b>	1159	1043	<b>515</b>	1136
	<u>NM_025019</u>	TUBA4	tubulin, alpha 4	1446	<b>1173</b>	1330	1477	<b>782</b>	1366
	<u>AK023150</u>		FLJ13088 fis, clone NT2RP3002102	798	<b>1087</b>	905	845	<b>564</b>	785
	<u>NM_017833</u>	C21orf55	Chromosome 21 open reading frame 55	741	<b>1079</b>	799	687	<b>508</b>	665
	<u>BC001407</u>		Similar to cytochrome c-like antigen	524	<b>1004</b>	629	506	<b>502</b>	577
	<u>AK023104</u>		FLJ22648 fis, clone HSI07329	441	<b>984</b>	621	488	<b>471</b>	495
	<u>AK024617</u>		FLJ20964 fis, clone ADSH00902	824	<b>955</b>	745	788	<b>535</b>	824
	<u>BC009536</u>		IMAGE:3892368	553	<b>924</b>	775	597	<b>498</b>	671
	<u>AK056287</u>		FLJ31725 fis, clone NT2RI2006716	435	<b>862</b>	907	405	<b>459</b>	893
	<u>AK021611</u>		FLJ11549 fis, clone HEMBA1002968	535	<b>812</b>	675	545	<b>392</b>	630
	<u>BC015119</u>		IMAGE:3951139	445	<b>784</b>	487	455	<b>435</b>	439
	<u>AK056492</u>		FLJ31930 fis, clone NT2RP7006162	252	<b>651</b>	525	266	<b>367</b>	457
	<u>AB058711</u>	KIAA1808	KIAA1808 protein	208	<b>637</b>	357	199	<b>339</b>	366
	<u>BC011266</u>		IMAGE:4156795	354	<b>632</b>	432	356	<b>328</b>	460
	<u>AK023316</u>		FLJ13254 fis, clone OVARC1000787	416	<b>596</b>	357	400	<b>290</b>	352
	<u>NM_024696</u>	FLJ23058	Hypothetical protein FLJ23058	456	<b>541</b>	346	436	<b>313</b>	359
	<u>AF253316</u>		Pheromone receptor (PHRET) pseudogene	136	<b>520</b>	425	128	<b>301</b>	347
	<u>AK056007</u>	BICD1	Bicaudal D homolog 1 (Drosophila)	704	<b>505</b>	439	624	<b>243</b>	305
	<u>AB020632</u>	KIAA0825	KIAA0825 protein	249	<b>498</b>	353	246	<b>272</b>	339
	<u>NM_017609</u>	DKFZp434A1721	Hypothetical protein DKFZp434A1721	182	<b>485</b>	319	190	<b>298</b>	304
	<u>NM_018190</u>	FLJ10715	Hypothetical protein FLJ10715	202	<b>483</b>	310	174	<b>206</b>	266
	<u>AK057046</u>		FLJ32484 fis, clone SKNM2001555	229	<b>473</b>	294	261	<b>302</b>	228
	<u>NM_013395</u>	AD013	Proteinx0008	448	<b>461</b>	496	403	<b>304</b>	378
	<u>BC008501</u>	MGC14839	Similar to RIKEN cDNA 2310030G06	379	<b>414</b>	329	443	<b>264</b>	290

**Table I: Differentially expressed genes between adult and cord monocytes at specific time points. T = time (min) at which the sample was taken. Numbers indicate corrected expression values. (Continued)**

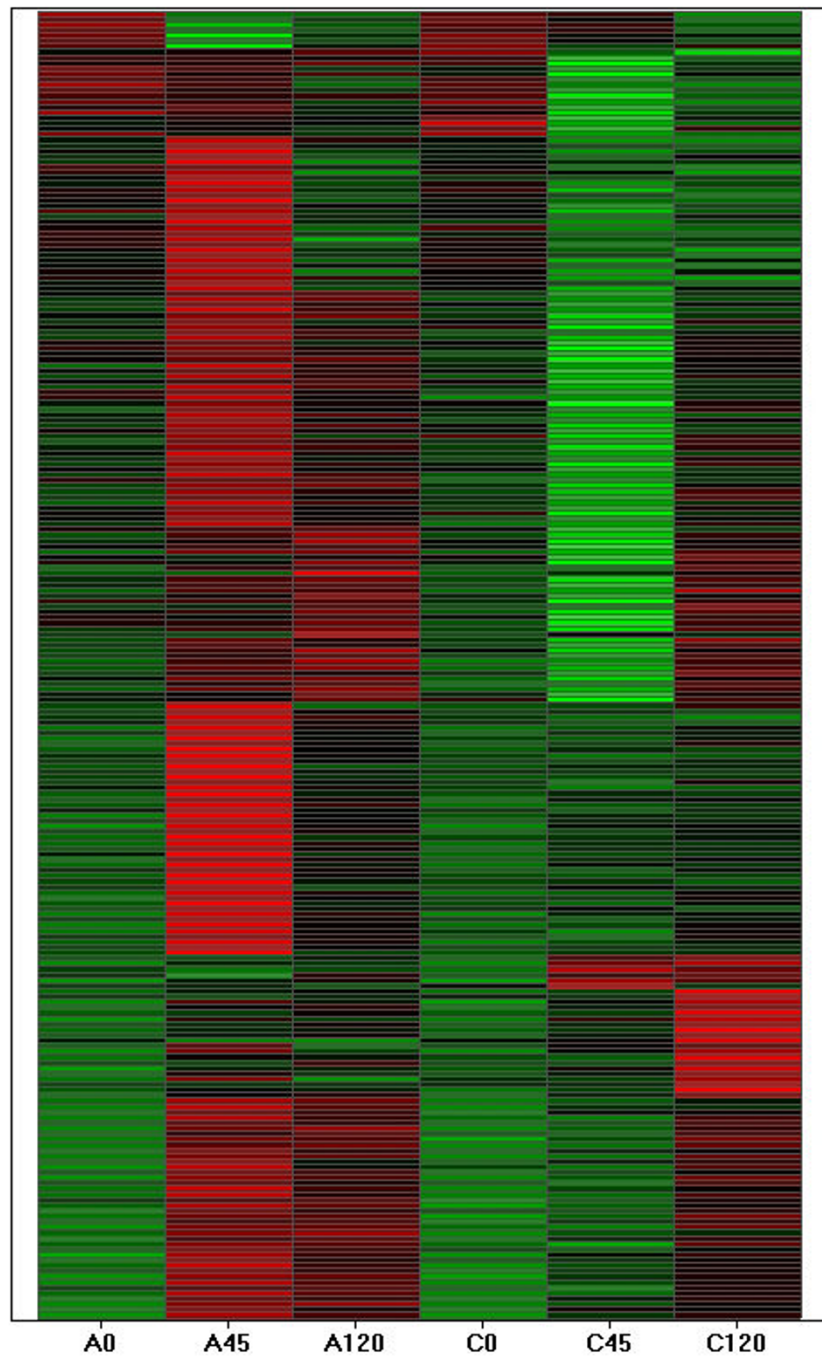
<u>AK021988</u>	FLJ11926 fis, clone HEMBB1000374	321	<b>411</b>	399	280	<b>218</b>	288
<u>AF119872</u>	PRO2272	257	<b>405</b>	327	257	<b>205</b>	250
<u>NM_022744</u>	FLJ13868	267	<b>376</b>	239	270	<b>212</b>	172
<u>AK022364</u>	FLJ12302 fis, clone MAMMA1001864	172	<b>355</b>	316	164	<b>184</b>	332
<u>BC002644</u>	MGC485 9	282	<b>335</b>	382	257	<b>223</b>	331
<u>AK022201</u>	FLJ12139 fis, clone MAMMA1000339	267	<b>302</b>	152	235	<b>123</b>	131
<u>NM_017953</u>	FLJ20729	170	<b>290</b>	258	138	<b>170</b>	218
<u>AK057473</u>	FLJ32911 fis, clone TESTI2006210	160	<b>268</b>	265	163	<b>123</b>	247
<u>U50383</u>	RAI15	206	<b>265</b>	236	198	<b>159</b>	186
<u>AK027027</u>	FLJ23374 fis, clone HEP16126	134	<b>261</b>	170	134	<b>152</b>	141
<u>AK057288</u>	FLJ32726 fis, clone TESTI2000981	206	<b>249</b>	312	216	<b>152</b>	244
<u>U79280</u>	PIPPIN	274	<b>229</b>	189	238	<b>117</b>	134
<u>AK023628</u>	FLJ13566 fis, clone PLACE1008330	140	<b>195</b>	230	133	<b>128</b>	193
<u>NM_025263</u>	CAT56	126	<b>194</b>	147	127	<b>101</b>	130
<u>AF311324</u>	Ubiquitin-like fusion protein	191	<b>189</b>	179	190	<b>106</b>	138
<u>NM_005708</u>	GPC6	107	<b>185</b>	144	109	<b>88</b>	146
<u>AB037778</u>	KIAA135 7	153	<b>180</b>	156	149	<b>118</b>	146
<u>AK055939</u>	FLJ31377 fis, clone NESOP1000087	152	<b>167</b>	179	136	<b>105</b>	173
<u>NM_018316</u>	FLJ11078	89	<b>145</b>	118	73	<b>94</b>	103
<u>AF402776</u>	BIC	82	<b>136</b>	171	96	<b>88</b>	153
<u>BC003416</u>	IMAGE:3450973	64	<b>133</b>	93	83	<b>73</b>	111
<u>AL137491</u>	DKFZp434P1530	62	<b>130</b>	88	57	<b>72</b>	74
<u>AK057770</u>	FLJ25041 fis, clone CBL03194	110	<b>130</b>	114	108	<b>83</b>	84
<u>AB058769</u>	KIAA186 6	89	<b>126</b>	122	102	<b>83</b>	91
<u>AB058747</u>	WAC	60	<b>124</b>	103	57	<b>76</b>	77
<u>AK054885</u>	C6orf31	51	<b>119</b>	108	41	<b>68</b>	119
<u>AK022235</u>	FLJ12173 fis, clone MAMMA1000696	109	<b>103</b>	94	90	<b>62</b>	77
<u>AK026853</u>	AOAH	59	<b>98</b>	64	59	<b>61</b>	56
<u>AK024877</u>	FLJ21224 fis, clone COL00694	53	<b>96</b>	110	55	<b>54</b>	103
<u>NM_003171</u>	SUPV3L1	65	<b>93</b>	60	60	<b>55</b>	58
<u>NM_052933</u>	TSGA13	66	<b>80</b>	70	68	<b>44</b>	71
<u>AK057907</u>	FLJ25178 fis, clone CBR09176	42	<b>77</b>	31	47	<b>43</b>	41
<u>AK055748</u>	FLJ31186 fis, clone KIDNE2000335	88	<b>67</b>	68	79	<b>44</b>	71
<u>BC013757</u>	IMAGE:4525041	40	<b>54</b>	39	43	<b>33</b>	32
<u>AL365511</u>	Novel human gene mapping to chromosome 22	19	<b>48</b>	29	20	<b>27</b>	37
<u>AK026889</u>	APRIN	31	<b>35</b>	42	34	<b>21</b>	34
<u>AK057423</u>	FLJ32861 fis, clone TESTI2003589	36	<b>32</b>	34	30	<b>18</b>	31
<u>AK055543</u>	MLSTD1	31	<b>31</b>	32	27	<b>18</b>	30
<u>AK056513</u>	FLJ31951 fis, clone NT2RP7007177	33	<b>29</b>	20	22	<b>13</b>	20
<u>NM_013319</u>	TEREI	22	<b>28</b>	19	24	<b>17</b>	22
<u>AK026456</u>	FLJ22803 fis, clone KAIA2685	15	<b>26</b>	14	16	<b>13</b>	17
<u>AK021610</u>	cDNA FLJ11548 fis, clone HEMBA1002944	34	<b>26</b>	29	31	<b>15</b>	28
<u>AK026823</u>	FLJ23170 fis, clone LNG09984	15	<b>22</b>	14	19	<b>8</b>	18
<u>AK056805</u>	FLJ32243 fis, clone PROST1000039	400	<b>177</b>	186	343	<b>314</b>	160
<u>NM_012238</u>	SIRT1	149	<b>156</b>	<b>170</b>	178	134	<b>109</b>
<u>NM_016099</u>	GOLGA7	10493	15165	<b>9882</b>	1194 7	11564	<b>15698</b>
<u>AK022482</u>	FLJ12420 fis, clone MAMMA1003049	6052	9099	<b>5803</b>	6362	7620	<b>9309</b>
<u>AK026490</u>	RAB32	3677	7044	<b>4641</b>	3671	5553	<b>7561</b>
<u>NM_020684</u>	NPD007	674	794	<b>764</b>	630	720	<b>1215</b>
<u>AL390158</u>	ATXN7L 3	319	460	<b>378</b>	339	403	<b>598</b>
<u>NM_017752</u>	FLJ20298	146	237	<b>282</b>	133	233	<b>493</b>
<u>AB037743</u>	KIAA132 2	236	202	<b>199</b>	239	246	<b>319</b>
<u>AF339819</u>	clone IMAGE:38177	77	111	<b>110</b>	96	125	<b>174</b>
<u>AK055215</u>	FLJ30653 fis, clone DFNES2000143	47	48	<b>58</b>	43	80	<b>92</b>

**Figure 1**

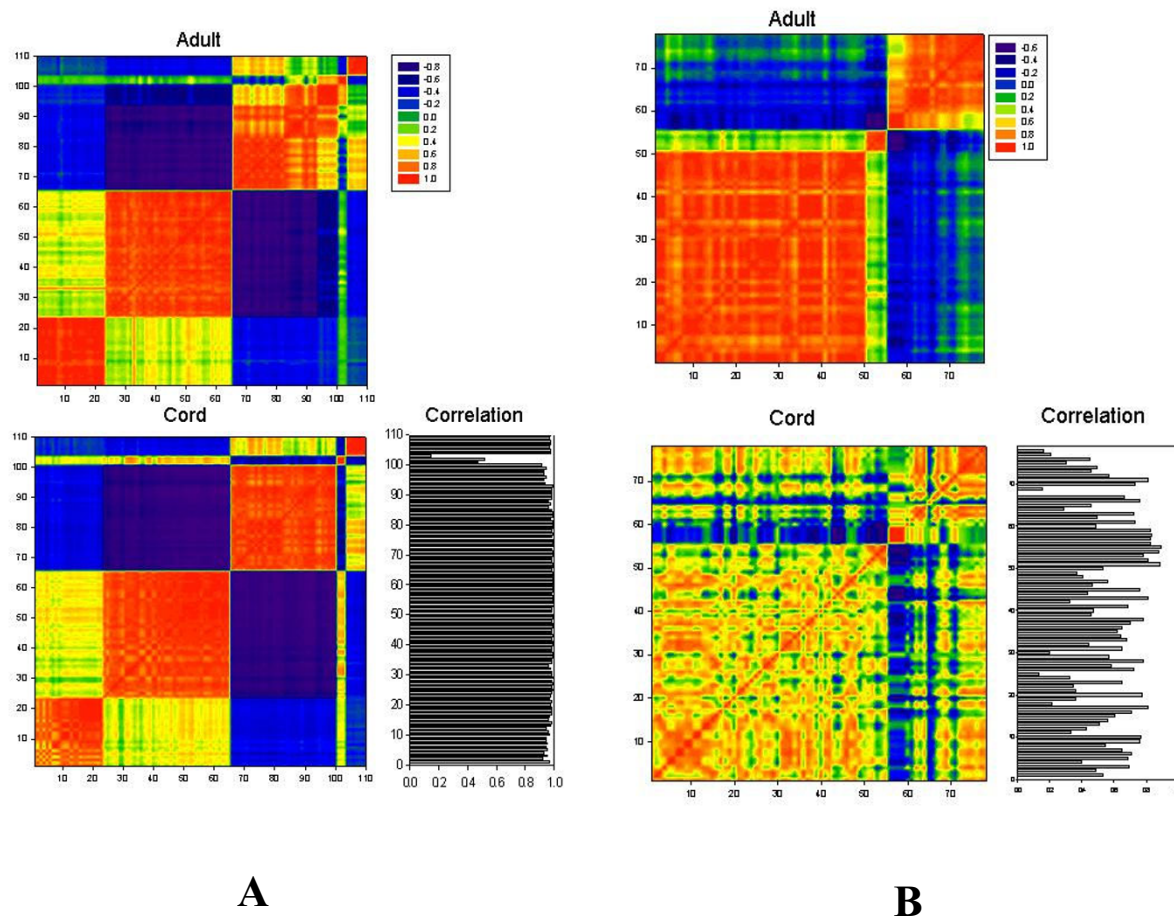
LPS-stimulated genes in cord blood and adult monocytes can be differentiated on the basis of kinetics of expression. Expression level (in relative intensity units) is shown of the y-axis and time on the x-axis. At the 45 min time point, significant differences in expression level were seen between adult and neonatal monocytes for each of the gene groups A-H.

between cells from these two groups, as measured by the correlation coefficients between genes from adult and cord monocytes with value > 0.90 (figure 3A, black and white graph to the right). Three genes on this list (#101–103) were the exception: transcriptional regulator interacting with the PHS-bromodomain 2 (*Trip-Br2*), interleukin 1 beta (*Il1b*), and the GRO2 oncogene(*Gro2*). These genes may play a critical role in differentiation between adult and cord monocyte behaviour [22,23]. The high similarity of these mosaics presents evidence for the presence of fundamental processes in monocyte development that appear to be quite similar in both groups of samples. The details of the genes used in Figure 3A are presented as Table 2. Another group of 78 genes were found that have different cluster designations between adult and cord blood monocytes (Figure 3B). Details of these genes are listed in Table 3.

We analyzed these genes using DFA in order to find those genes most likely to highlight the differences between cord and adult monocytes. DFA identified genes having high discriminatory capabilities. The DFA software selected genes from Table 3 with highest discriminatory capabilities for this case. A total of 12 genes (marked with asterisk in Table 3) were used by the DFA program to differentiate dynamical changes in both cord and adult monocytes after LPS stimulation. Values of the roots obtained by DFA analysis were used to graphically depict the differences of the gene expression values obtained in cord and adult samples in different stages after stimulation (Fig. 4). The spatial organization of the elements in this representation provides a measure of the overall similarity of the dynamic behaviour of these samples. The greatest temporal changes in gene expression noted above after 45 min of LPS expo-

**Figure 2**

Heat map representation of differences in gene expression of adult and cord blood monocytes in response to LPS. Z-transformed scores of the mean expression values for adult monocytes prior to (A0), after 45 min (A45), and after 120 min (A120) of LPS exposure are graphically shown to the left. Similar scores from cord blood monocytes prior to (C0), after 45 min (C45), and after 120 min (C120) of LPS exposure, respectively. The heat map was produced using software from Spotfire Decision Site (Somerville, MA).

**Figure 3**

Correlative mosaic for genes selected as HV-genes in cord blood and adult monocytes, belonging to five clusters of highest content. A. Genes of the same cluster in cord and adult; B. Genes of different cluster in cord and adult. Correlation coefficients are color-coded according to the key in the upper right. The correlation between the adult and cord blood monocyte profiles for each gene are shown in black and white, lower right.

sure were also observed in the analysis using these 12 genes. However, almost no differences occurred at the 2 hr time point between cord and adult cells suggesting that the global behavior of the cells is similar, but the kinetics of change differ i.e. many of the changes are the same in both groups, but they occur at different rates.

#### **Apoptosis assays**

The products of a subset of genes that were differentially expressed between groups after 45 min exposure to LPS are involved in apoptosis. We therefore performed a series of functional experiments comparing apoptosis in adult ( $n = 10$ ) and neonatal ( $n = 10$ ) cord bloods. Results of these assays are shown in Table 4. Annexin assays demonstrated that adult monocytes display different kinetics for both apoptosis and necrosis as compared with neonatal

monocytes. Flow cytometry revealed that  $43 \pm 5\%$  (mean  $\pm$  SD) of adult and  $53 \pm 8\%$  of neonatal monocytes are undergoing apoptosis after stimulation with LPS for 14 hours ( $p < 0.002$ ), while  $38 \pm 8\%$  of adult and  $25 \pm 9\%$  of neonatal monocytes are necrotic after 14 hours of LPS stimulation ( $p < 0.003$ ). The number of live monocytes after 14 hours of LPS stimulation was not statistically different between the two groups. There was also no statistically significant difference in the number of live, apoptotic, or necrotic monocytes between adult and neonatal samples prior to LPS stimulation (data not shown).

#### **Discussion**

Following a given physiologic stimulus, signalling kinase activation, transcription factor translocation, and gene transcription all occur in rapid order. However, like all

**Table 2: Genes from which correlation mosaics in Figure 3A were derived. Genes in this table show the highest level of correlation by DFA analysis comparing adult and cord blood monocytes.**

Order in mosaic	Accession No.	Gene symbol	Description
1	<a href="#">NM_017614</a>	BHMT2	Betaine-homocysteine methyltransferase 2
2	<a href="#">NM_001651</a>	AQP5	Aquaporin 5
3	<a href="#">NM_020163</a>	LOC56920	Semaphorin sem2
4	<a href="#">NM_012343</a>	NNT	Nicotinamide nucleotide transhydrogenase
5	<a href="#">NM_000096</a>	CP	Ceruloplasmin (ferroxidase)
6	<a href="#">NM_005819</a>	STX6	Syntaxin 6
7	<a href="#">NM_052951</a>	C20orf167	Chromosome 20 open reading frame 167
8	<a href="#">NM_001348</a>	DAPK3	Death-associated protein kinase 3
9	<a href="#">X73502</a>	KRT20	Cytokeratin 20
10	<a href="#">NM_052887</a>	TIRAP	Toll-interleukin 1 receptor (TIR) domain-containing adapter protein
11	<a href="#">NM_019555</a>	ARHGEF3	Rho guanine nucleotide exchange factor (GEF) 3
12	<a href="#">NM_014380</a>	NGFRAP1	Nerve growth factor receptor (TNFRSF16) associated protein 1
13	<a href="#">NM_001272</a>	CHD3	Chromodomain helicase DNA binding protein 3
14	<a href="#">NM_005842</a>	SPRY2	Sprouty homolog 2 (Drosophila)
15	<a href="#">NM_012332</a>	MT-ACT48	Mitochondrial Acyl-CoA Thioesterase
16	<a href="#">BC015041</a>	VATI	Vesicle amine transport protein 1
17	<a href="#">NM_003872</a>	NRP2	Neuropilin 2
18	<a href="#">NM_005849</a>	IGSF6	Immunoglobulin superfamily, member 6
19	<a href="#">NM_014323</a>	ZNF278	Zinc finger protein 278
20	<a href="#">NM_030674</a>	SLC38A1	Solute carrier family 38, member 1
21	<a href="#">NM_004153</a>	ORC1L	Origin recognition complex, subunit 1-like (yeast)
22	<a href="#">NM_005249</a>	FOXP1B	Forkhead box G1B
23	<a href="#">NM_021048</a>	MAGEA10	Melanoma antigen, family A, 10
24	<a href="#">M60502</a>	FLG	Filaggrin
25	<a href="#">NM_004997</a>	MYBPH	Myosin binding protein H
26	<a href="#">J05046</a>	INSRR	Insulin receptor-related receptor
27	<a href="#">M33987</a>	CA1	Carbonic anhydrase 1
28	<a href="#">D31886</a>	RAB3GAP	RAB3 GTPase-ACTIVATING PROTEIN
29	<a href="#">L24498</a>	GADD45A	Growth arrest and DNA-damage-inducible, alpha
30	<a href="#">L07590</a>	PPP2R3	Protein phosphatase 2 (formerly 2A), regulatory subunit B" (PR 72), alpha isoform and (PR 130), bet
31	<a href="#">D87024</a>	IGLV4-3	Immunoglobulin lambda variable 4-3
32	<a href="#">L35848</a>	MS4A3	Membrane-spanning 4-domains, subfamily A, member 3 (hematopoietic cell-specific)
33	<a href="#">M18216</a>	CEACAM6	Carcinoembryonic antigen-related cell adhesion molecule 6 (non-specific cross reacting antigen)
34	<a href="#">M11952</a>	TRBV7-8	T cell receptor beta variable 7-8
35	<a href="#">D89094</a>	PDE5A	Phosphodiesterase 5A, cGMP-specific
36	<a href="#">M77140</a>	GAL	Galanin
37	<a href="#">D13628</a>	ANGPT1	Angiopoietin 1
38	<a href="#">M81635</a>	EPB72	Erythrocyte membrane protein band 7.2 (stomatin)
39	<a href="#">D89859</a>	ZFP161	Zinc finger protein 161 homolog (mouse)
40	<a href="#">D26069</a>	CENTB2	Centaurin, beta 2
41	<a href="#">L10717</a>	ITK	IL2-inducible T-cell kinase
42	<a href="#">L04282</a>	ZNF148	Zinc finger protein 148 (pHZ-52)
43	<a href="#">L41944</a>	IFNAR2	Interferon (alpha, beta and omega) receptor 2
44	<a href="#">M82882</a>	ELFI	E74-like factor 1 (ets domain transcription factor)
45	<a href="#">L26339</a>	RCD-8	Autoantigen
46	<a href="#">D87328</a>	HLCS	Holocarboxylase synthetase (biotin-[proprionyl-Coenzyme A-carboxylase (ATP-hydrolysing)] ligase)
47	<a href="#">D00943</a>	MYH6	Myosin, heavy polypeptide 6, cardiac muscle, alpha (cardiomyopathy, hypertrophic 1)
48	<a href="#">D00099</a>	ATPIA1	ATPase, Na+/K+ transporting, alpha 1 polypeptide
49	<a href="#">L36531</a>	ITGA8	Integrin, alpha 8
50	<a href="#">D42084</a>	METAPI	Methionyl aminopeptidase 1
51	<a href="#">M76766</a>	GTF2B	General transcription factor IIB
52	<a href="#">J04621</a>	SDC2	Syndecan 2 (heparan sulfate proteoglycan 1, cell surface-associated, fibroglycan)
53	<a href="#">D31888</a>	RCOR	REST corepressor
54	<a href="#">L32832</a>	ATBF1	AT-binding transcription factor 1

**Table 2: Genes from which correlation mosaics in Figure 3A were derived. Genes in this table show the highest level of correlation by DFA analysis comparing adult and cord blood monocytes. (Continued)**

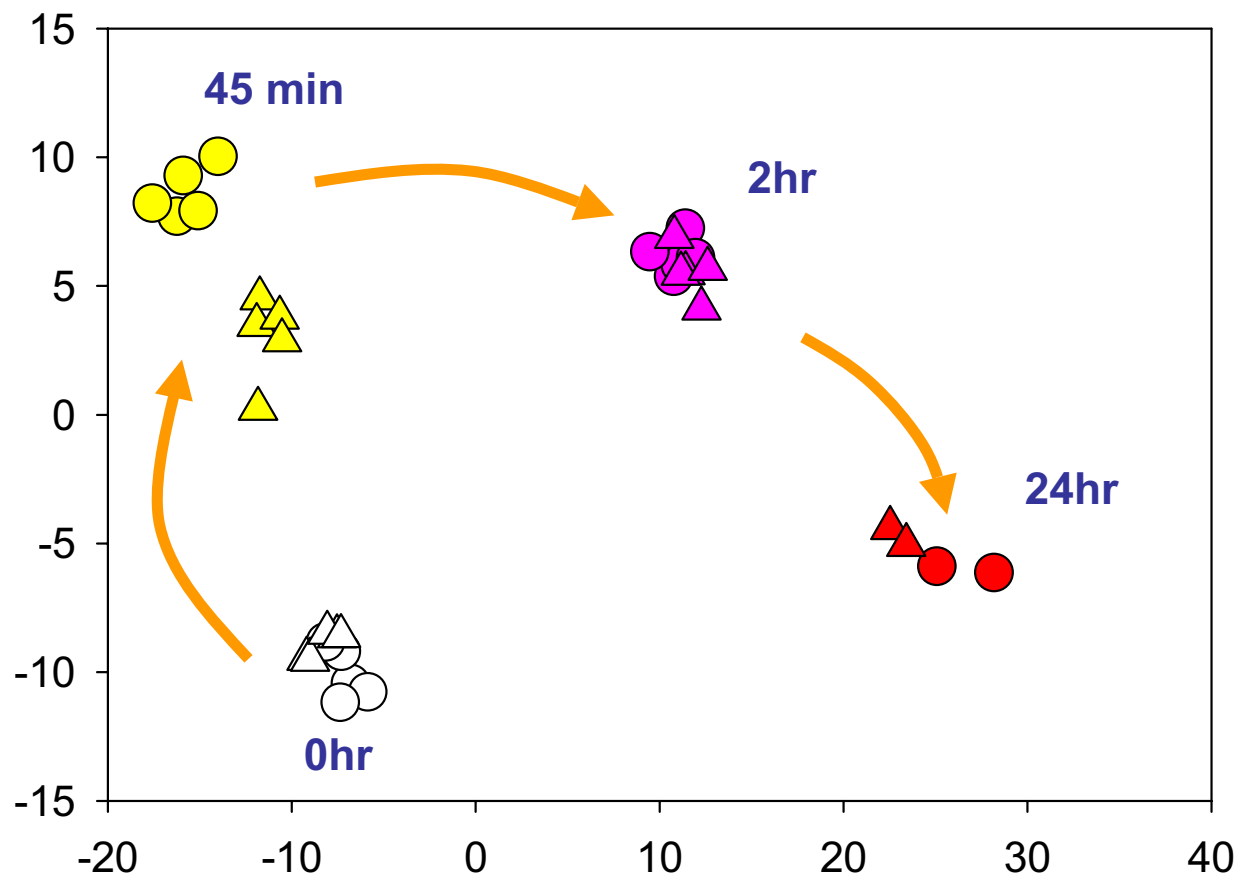
55	<u>D86981</u>	APPBP2	Amyloid beta precursor protein (cytoplasmic tail) binding protein 2
56	<u>M94362</u>	LMNB2	Lamin B2
57	<u>M54968</u>	KRAS2	V-Ki-ras2 Kirsten rat sarcoma 2 viral oncogene homolog
58	<u>D42046</u>	DNA2L	DNA2 DNA replication helicase 2-like (yeast)
59	<u>D86964</u>	DOCK2	Dedicator of cyto-kinesis 2
60	<u>D50683</u>	TGFBR2	Transforming growth factor, beta receptor II (70–80 kD)
61	<u>M96843</u>	ID2B	Striated muscle contraction regulatory protein
62	<u>M61906</u>	PIK3R1	Phosphoinositide-3-kinase, regulatory subunit, polypeptide 1 (p85 alpha)
63	<u>M12679</u>	HUMMHCW1A	Cwl antigen
64	<u>M63623</u>	OMG	Oligodendrocyte myelin glycoprotein
65	<u>J04162</u>	FCGR3B	Fc fragment of IgG, low affinity IIIb, receptor for (CD16)
66	<u>L48516</u>	PON3	Paraoxonase 3
67	<u>M54927</u>	PLPI	Proteolipid protein 1 (Pelizaeus-Merzbacher disease, spastic paraplegia 2, uncomplicated)
68	<u>D86973</u>	GCN1LI	GCN1 general control of amino-acid synthesis 1-like 1 (yeast)
69	<u>D43968</u>	RUNX1	Runt-related transcription factor 1 (acute myeloid leukemia 1-amll oncogene)
70	<u>L05500</u>	ADCY1	Adenylate cyclase 1 (brain)
71	<u>D80010</u>	LPINI	Lipin 1
72	<u>D50918</u>	SEPT6	Septin 6
73	<u>D86988</u>	RENT1	Regulator of nonsense transcripts 1
74	<u>M90391</u>	IL16	Interleukin 16 (lymphocyte chemoattractant factor)
75	<u>M62324</u>	MRF-1	Modulator recognition factor 1
76	<u>L77565</u>	DGS-H	DiGeorge syndrome gene H
77	<u>D86970</u>	TIAFI	TGFBI-induced anti-apoptotic factor 1
78	<u>D38169</u>	ITPKC	Inositol 1,4,5-trisphosphate 3-kinase C
79	<u>D87684</u>	UBXD2	UBX domain-containing 2
80	<u>D84454</u>	SLC35A2	Solute carrier family 35 (UDP-galactose transporter), member 2
81	<u>M97496</u>	GUCA2A	Guanylate cyclase activator 2A (guanylin)
82	<u>M95585</u>	HLF	Hepatic leukemia factor
83	<u>L38517</u>	IHH	Indian hedgehog homolog (Drosophila)
84	<u>L20860</u>	GPIBB	Glycoprotein Ib (platelet), beta polypeptide
85	<u>M26880</u>	UBC	Ubiquitin C
86	<u>D86962</u>	GRB10	Growth factor receptor-bound protein 10
87	<u>D63481</u>	SCRIB	Scribble
88	<u>D17525</u>	MASPI	Mannan-binding lectin serine protease 1 (C4/C2 activating component of Ra-reactive factor)
89	<u>L26584</u>	RASGRF1	Ras protein-specific guanine nucleotide-releasing factor 1
90	<u>M65066</u>	PRKAR1B	Protein kinase, cAMP-dependent, regulatory, type I, beta
91	<u>J05158</u>	CPN2	Carboxypeptidase N, polypeptide 2, 83 kD
92	<u>L36861</u>	GUCA1A	Guanylate cyclase activator 1A (retina)
93	<u>L11239</u>	GBX1	Gastrulation brain homeo box 1
94	<u>D90145</u>	SCYA3LI	Small inducible cytokine A3-like 1
95	<u>M96739</u>	NHLH1	Nescient helix loop helix 1
96	<u>M12959</u>	TRA@	T cell receptor alpha locus
97	<u>D80005</u>	C9orf10	C9orf10 protein
98	<u>M13231</u>	TRGC2	T cell receptor gamma constant 2
99	<u>D28588</u>	SP2	Sp2 transcription factor
100	<u>M57732</u>	TCFI	Transcription factor 1, hepatic-LF-B1, hepatic nuclear factor (HNF1), albumin proximal factor
101	<u>NM_014755</u>	TRIP-Br2	Transcriptional regulator interacting with the PHS-bromodomain 2
102	<u>NM_000576</u>	IL1B	Interleukin 1, beta
103	<u>NM_002089</u>	GRO2	GRO2 oncogene
104	<u>NM_002089x</u>	GPCR5D	G protein-coupled receptor, family C, group 5, member D
105	<u>NM_002713</u>	PPP1R8	Protein phosphatase 1, regulatory (inhibitor) subunit 8
106	<u>NM_014383</u>	TZFP	Testis zinc finger protein
107	<u>NM_012248</u>	SPS2	Selenophosphate synthetase 2
108	<u>AL137438</u>	SEC15L	SEC15 ( <i>S. cerevisiae</i> )-like
109	<u>NM_005387</u>	NUP98	Nucleoporin 98 kD
110	<u>NM_003476</u>	CSRP3	Cysteine and glycine-rich protein 3 (cardiac LIM protein)

**Table 3: Genes from which the mosaic in Figure 3B were derived. Genes from which correlation mosaics in Figure 3B were derived. Genes in this table show the greatest differences by DFA analysis comparing adult and cord blood monocytes.**

Order in Mosaic	Accession No.	Gene Symbol	Description
1	<a href="#">AK055855</a>	CLDN10	Claudin 10
2	<a href="#">NM_000565</a>	IL6R	Interleukin 6 receptor
3	<a href="#">NM_006150</a>	LMO6	LIM domain only 6
4	<a href="#">NM_022787</a>	NMNAT	NMN adenylyltransferase-nicotinamide mononucleotide adenylyl transferase
5	<a href="#">NM_002743</a>	PRKCSH	Protein kinase C substrate 80K-H
6	<a href="#">NM_004847</a>	AIFI	Allograft inflammatory factor 1
7	<a href="#">NM_021073</a>	BMP5	Bone morphogenetic protein 5
* 8	<a href="#">AK025306</a>	CLK1	CDC-like kinase 1
9	<a href="#">NM_004280</a>	EEF1E1	Eukaryotic translation elongation factor 1 epsilon 1
* 10	<a href="#">NM_004432</a>	ELAVL2	ELAV (embryonic lethal, abnormal vision, Drosophila)-like 2 (Hu antigen B)
11	<a href="#">NM_012181</a>	FKBP8	FK506 binding protein 8 (38 kD)
12	<a href="#">NM_002091</a>	GRP	Gastrin-releasing peptide
13	<a href="#">NM_016355</a>	LOC51202	Hqp0256 protein
14	<a href="#">NM_021204</a>	MASA	E-1 enzyme
15	<a href="#">NM_004204</a>	PIGQ	Phosphatidylinositol glycan, class Q
16	<a href="#">NM_002928</a>	RGS16	Regulator of G-protein signalling 16
17	<a href="#">NM_005839</a>	SRRM1	Serine/arginine repetitive matrix 1
18	<a href="#">NM_003166</a>	SULT1A3	Sulfotransferase family, cytosolic, 1A, phenol-preferring, member 3
19	<a href="#">NM_000356</a>	TCOF1	Treacher Collins-Franceschetti syndrome 1
20	<a href="#">NM_016437</a>	TUBG2	Tubulin, gamma 2
* 21	<a href="#">NM_022568</a>	ALDH8A1	Aldehyde dehydrogenase 8 family, member A1
22	<a href="#">AF209930</a>	CHRD	Chordin
23	<a href="#">NM_005274</a>	GNG5	Guanine nucleotide binding protein (G protein), gamma 5
24	<a href="#">NM_018384</a>	IAN4L1	Immune associated nucleotide 4 like 1 (mouse)
25	<a href="#">NM_000640</a>	IL13RA2	Interleukin 13 receptor, alpha 2
26	<a href="#">AK021692</a>	LOC51141	Insulin induced protein 2
27	<a href="#">NM_012443</a>	SPAG6	Sperm associated antigen 6
28	<a href="#">NM_003155</a>	STCI	Stanniocalcin 1
29	<a href="#">NM_022003</a>	FXYD6	FXYD domain-containing ion transport regulator 6
30	<a href="#">NM_002763</a>	PROX1	Prospero-related homeobox 1
31	<a href="#">NM_002836</a>	PTPRA	Protein tyrosine phosphatase, receptor type, A
32	<a href="#">AL136835</a>	TOLLIP	Toll-interacting protein
33	<a href="#">AB058691</a>	ALX4	Aristaless-like homeobox 4
34	<a href="#">AF112345</a>	ITGA10	Integrin, alpha 10
35	<a href="#">NM_022788</a>	P2RY12	Purinergic receptor P2Y, G protein-coupled, 12
36	<a href="#">NM_001213</a>	Clorf1	Chromosome 1 open reading frame 1
37	<a href="#">NM_005860</a>	FSTL3	Follistatin-like 3 (secreted glycoprotein)

**Table 3: Genes from which the mosaic in Figure 3B were derived. Genes from which correlation mosaics in Figure 3B were derived. Genes in this table show the greatest differences by DFA analysis comparing adult and cord blood monocytes. (Continued)**

38	<u>NM_013320</u>	HCF-2	Host cell factor 2
39	<u>NM_058246</u>	LOC136442	Similar to MRJ gene for a member of the DNAJ protein family
40	<u>NM_020169</u>	LXN	Latexin protein
41	<u>BC008993</u>	MGC17337	Similar to RIKEN cDNA 5730528L13 gene
42	<u>BC002712</u>	MYCN	V-myc myelocytomatosis viral related oncogene, neuroblastoma derived (avian)
43	<u>AK026164</u>	MYL6	Myosin, light polypeptide 6, alkali, smooth muscle and non-muscle
44	<u>NM_006215</u>	SERPINA4	Serine (or cysteine) proteinase inhibitor, clade A (alpha-1 antiproteinase, antitrypsin), member 4
45	<u>NM_004790</u>	SLC22A6	Solute carrier family 22 (organic anion transporter), member 6
46	<u>NM_022911</u>	SLC26A6	Solute carrier family 26, member 6
47	<u>NM_003374</u>	VDAC1	Voltage-dependent anion channel 1
48	<u>NM_017818</u>	WDR8	WD repeat domain 8
49	<u>NM_003416</u>	ZNF7	Zinc finger protein 7 (KOX 4, clone HF.16)
50	<u>NM_002313</u>	ABLM	Actin binding LIM protein
51	<u>NM_012074</u>	CERD4	Cer-d4 (mouse) homolog
52	<u>NM_000787</u>	DBH	Dopamine beta-hydroxylase (dopamine beta-monooxygenase)
* 53	<u>NM_000561</u>	GSTM1	Glutathione S-transferase M1
54	<u>BC014075</u>	GTPBP1	GTP binding protein 1
55	<u>NM_033260</u>	HFH1	Winged helix/forkhead transcription factor
56	<u>NM_033033</u>	KRTHB2	Keratin, hair, basic, 2
57	<u>NM_004789</u>	LHX2	LIM homeobox protein 2
58	<u>NM_014106</u>	PRO1914	PRO1914 protein
* 59	<u>NM_006799</u>	PRSS21	Protease, serine, 21 (testisin)
* 60	<u>NM_002900</u>	RBP3	Retinol binding protein 3, interstitial
61	<u>NM_033022</u>	RPS24	Ribosomal protein S24
* 62	<u>AB029021</u>	TRIM35	Tripartite motif-containing 35
* 63	<u>NM_020989</u>	CRYGC	Crystallin, gamma C
* 64	<u>BI198124</u>	HMG1L10	High-mobility group (nonhistone chromosomal) protein 1-like 10
65	<u>NM_014163</u>	HSPC073	HSPC073 protein
66	<u>AF181985</u>	JIK	STE20-like kinase
67	<u>NM_017607</u>	PPPIR12C	Protein phosphatase 1, regulatory (inhibitor) subunit 12C
* 68	<u>NM_002873</u>	RAD17	RAD17 homolog ( <i>S. pombe</i> )
69	<u>NM_022095</u>	ZNF335	Zinc finger protein 335
* 70	<u>M90355</u>	BTF3L2	Basic transcription factor 3, like 2
71	<u>NM_002079</u>	GOT1	Glutamic-oxaloacetic transaminase 1, soluble (aspartate aminotransferase 1)
72	<u>NM_004146</u>	NDUFB7	NADH dehydrogenase (ubiquinone) 1 beta subcomplex, 7 (18 kD, B18)
73	<u>L38486</u>	MFAP4	Microfibrillar-associated protein 4
* 74	<u>AF111848</u>	ACTB	Actin, beta
75	<u>NM_001916</u>	CYCI	Cytochrome c-1

**Figure 4**

DFA analysis of phases of monocyte activation comparing cord and adult cells. DFA identified a subset of genes (see Table 3) whose expression values can be linearly combined in an equation, denoted a root, whose overall value is distinct for a given characterized group. These roots used as coordinate for presentation of these groups of samples in scatterplot. Results from individual samples for adult monocyte (circles) and cord monocytes (triangles) are discussed in the text. Results from individual samples for adult monocyte (circles) and cord monocytes (triangles) are shown.

biological processes, mRNA accumulation (or decreases) does not occur uniformly, and we hypothesized that examining the kinetics of mRNA accumulation or disappearance might provide clues into relevant cellular dynamics. We used a well-developed and validated gene expression microarray to examine the dynamics of mRNA accumulation and differences between adult and neonatal monocytes in that process.

Genes were found to be differentially expressed between adult and cord monocytes after either 45 or 120 minutes of LPS exposure, with little difference at 24 hr (see Figure 4). Interestingly, no statistically significant differences in gene expression were observed between these groups in untreated cells. Previous reports by others indicated

altered functions of cord blood monocytes in cytokine secretion and cellular adhesion. Results from this study cast new light on these findings and add complexity to understanding such differences. In some cases, our data support previous speculations about neonatal immune function. For example, the increased expression of IL-17B in neonatal monocytes is consistent with the observations of Vanden Eijnden and colleagues that newborns compensate for their relative immune deficiency by over-expression of the IL23-IL-17 signalling pathway in dendritic cells [24]. Similarly, we found significant elevations in cord monocyte transcripts of the chemokines MIP1B and MIP1A after 2 hrs of LPS exposure, consistent with Sullivan and colleagues' report of higher amounts of MIP $\alpha$  in cord blood samples compared with adults [25].

**Table 4: Results of Annexin Binding Assays**

Cell Type	Apoptotic Cells	Necrotic Cells	Significance
Adult monocytes	43 ± 5%	38 % ± 8%	P < 0.002
Cord blood monocytes	53 ± 8%	25% ± 9%	P < 0.003

On the other hand, transcripts for cadherin 9, *Rock1*, periostin, heparin sulfate 6-O-sulfotransferase 3, and C20orf42, whose products participate in various mechanisms that are associated with adhesion [26-28] were statistically significantly increased in adult monocytes after 45 min of LPS exposure, although no differences in expression for these genes between groups were detected at the later time point. These data suggest complex, dynamic relations for genes whose products are associated with cellular adhesion, and collectively highlight the importance of examining gene expression profiles (or related protein expression levels) over time.

The limits of gene expression profiling as a technique, albeit a very useful technique, must be acknowledged. The technique examines only RNA transcripts, not protein synthesis. Thus, alterations in other critical inflammatory mediators, such as eicosanoids, remain unobserved with this method. Furthermore, it is well known that there are many proteins, including critical inflammatory mediators, whose synthesis and secretion is not directly related in mRNA accumulation [29]. Thus, gene expression profiling should be complemented with other methods in order to maximize there potential.

In the final analysis, the utility of gene expression profiling will be demonstrated only if they provide insights into relevant physiologic or pathophysiologic function. For that reason, we elected to test the validity of the array data by examining a physiologic mechanism implicated by computer modelling of the array data. As noted in Table 1, adult monocytes over-expressed a small number of genes associated with the regulation of apoptosis. Since monocyte activation is a "balancing act" between signals inducing apoptosis and those inducing activation and differentiation [30,31], differences in the kinetics of expression or activation of enzymes or transcription factors that regulate apoptosis could have a crucial outcome on whether monocyte responses are pro- or anti-inflammatory. Annexin assays confirmed that there are significant differences in the appearance of apoptotic cells between adults and newborn monocytes (Table 4). Since apoptotic cells dampen the inflammatory response, it is interesting to speculate that the related blunted neonatal response to inflammatory stimuli (including infection) may result, at least in part, from the excessive production of apoptotic cells during monocyte activation.

There has been, to our knowledge, one previously published paper using gene expression arrays to study neonatal monocyte function [14]. Our findings differ somewhat from those described by these authors. The most obvious difference was our finding of no statistically significant differences between adult and cord blood samples in the resting state. We should note, however, that it is otherwise difficult to compare the two studies. Jiang and colleagues used a 1000-fold greater dose of LPS to stimulate the monocytes, and RNA was prepared after 18 hr of stimulation. Thus, it is difficult to determine which of the effects observed by these authors were the direct result of LPS activation or were mediated through autocrine activation by proteins secreted in response to LPS. Furthermore, the non-physiologic dose of LPS used by those authors makes the biological/pathological relevance of that study difficult to interpret. Finally, we should note that the study by Jiang and colleagues used different methodologies for purifying monocytes. While our method, positive selection using CD14-coated microbeads, carries the theoretical risk of activating the cells through TLR-4/CD14 signaling pathways, adherence procedures carry the greater risk of activating the cells, as β2 integrins are activated during the adherence process.

From the bioinformatics standpoint, our data demonstrate how gene microarray experiments can quickly move from the generation of gene lists to the development of plausible and testable models of relevant biology and physiology. Specifically, they demonstrate that computer-assisted, physiologic modelling is another means of corroborating array findings and provides the advantage of providing an approach for immediately testing the biological relevance of microarray data before embarking on the sometimes laborious task of confirming differential expression of dozens or even hundreds of genes identified in a microarray experiment. As described in the results section, the differences between groups in gene expression at 45 min were attributable to a unique up-regulation of specific genes in adult monocytes, a unique down-regulation of other genes in cord monocytes, or a combination of both processes for other genes. We have searched for mechanisms that account for these patterns. Specifically, we have analyzed the genes within derived k-means clusters to determine if a large number of genes within a cluster are related to overlapping functions using Ingenuity Pathway Assist software, or alternatively to shared transcriptional response elements upstream of these genes.

However, these strategies have failed to elucidate reasons to explain these findings.

Our studies also suggest that, while expensive and time-consuming to undertake, studying the kinetics of gene expression using microarrays can be highly informative. The previously reported study [14] examining gene expression differences between adult and cord blood monocytes was performed at only a single time point (18 hr after activation with a non-physiologic dose of LPS). Our studies suggest that the relevant biology may lie not in the specific genes that are differentially expressed at one particular time point, but, as one would predict with a dynamic system, which genes are expressed when. Timing of mRNA accumulation could determine, among other things, whether pro-apoptotic signals are processed in monocytes before cellular necrosis ensues.

The validity of the dynamic/kinetic approach is further supported by the correlation analyses (Figures 3 and 4). These analyses demonstrate clearly that the accumulation of a specific mRNA is not an independent event. Gene transcription and mRNA degradation are dynamic processes closely tied to the accumulation or degradation of other mRNAs and the transcription of their cognate proteins. We contend that, without this dynamic view of cellular activity, investigators attempting to use microarray data to elucidate relevant biological or pathological processes will encounter unnecessary obstacles in attempts to move from the generation of gene lists to testing specific hypotheses.

## Abbreviations

LPS – Lipopolysaccharide

DFA – Discriminant function analysis

HV – Hypervariable

## Acknowledgements

Supported in part by the National Institutes of Health (NIH), National Center for Research Resources, a component of the NIH, General Clinical Research Center Grant MO1 RR-14467, NIH grants P20 RR020143-01, P20 RR15577, P20 RR17703, and P20 R016478-04 and by the Oklahoma Center for Science and Technology (OCAST).

The authors also wish to extend their thanks to Julie McGhee, M.D., for her review and thoughtful comments on this manuscript.

## References

- Kobayashi S, Ohnuma K, Uchiyama M, Iino K, Iwata S, Dang NH, Morimoto C: **Association of CD26 with CD45RA outside lipid rafts attenuates cord blood T-cell activation.** *Blood* 2004, **103**:1002-1010.
- Adkins B, LeClerc C, Marshall-Clark S: **Neonatal adaptive immunity comes of age.** *Nature Rev Immunol* 2004, **4**:553-564.
- Garcia AM, Fadel SA, Cao S, Sarzotti M: **T cell immunity in neonates.** *Immunol Res* 2000, **22**:177-190.
- Zhao Y, Dai ZP, Lv P, Gao XM: **Phenotypic and functional analysis of human T lymphocytes in early second- and third-trimester fetuses.** *Clin Exp Immunol* 2002, **129**:302-308.
- Zola H, Fusco M, Weedon H, Macardle PJ, Ridings J, Robertson DM: **Reduced expression of the interleukin-2-receptor gamma chain on cord blood lymphocytes: relationship to functional immaturity of the neonatal immune response.** *Immunol* 1996, **87**:86-91.
- Schuit KE, Powell DA: **Phagocytic dysfunction in monocytes of normal newborn infants.** *Pediatrics* 1980, **65**:501-504.
- Tan ND, Davidson D: **Comparative differences and combined effects of interleukin-8, leukotriene B<sub>4</sub>, and platelet-activating factor on neutrophil chemotaxis of the newborn.** *Pediatr Res* 1995, **38**:11-16.
- Anderson DC, Hughes BJ, Smith CW: **Abnormal mobility of neonatal polymorphonuclear leukocytes.** *J Clin Invest* 1981, **68**:863-874.
- Anderson DC, Freeman KLB, Heerdt B, Hughes BJ, Jack RM, Smith CW: **Abnormal stimulated adherence of neonatal granulocytes: impaired induction of surface Mac-1 by chemotactic factors or secretagogues.** *Blood* 1987, **70**:740-750.
- Torok C, Lundahl J, Hed J, Lagercrantz H: **Diversity of regulation of adhesion molecules (Mac-1 and L-selectin) in monocytes and neutrophils from neonates and adults.** *Arch Dis Child* 1993, **68**:561-565.
- Hariharan D, Ho W, Cutilli J, Campbell DE, Douglas SD: **C-C chemokine profile of cord blood mononuclear cells: selective defect in RANTES production.** *Blood* 2000, **95**:715-718.
- Bessler H, Mendel C, Straussberg R, Gurary N, Aloni D, Sirota L: **Effects of dexamethasone on IL-1beta, IL-6, and TNF-alpha production by mononuclear cells of newborns and adults.** *Biol Neonate* 1999, **75**:225-233.
- Kotiranta-Ainamo A, Rautonen J, Rautonen N: **Interleukin-10 production by cord blood mononuclear cells.** *Pediatric Res* 1997, **41**:110-113.
- Jiang H, Van de Ven C, Satwani P, Baxi LV, Cairo MS: **Differential gene expression patterns by oligonucleotide microarray of basal versus lipopolysaccharide-activated monocytes from cord blood versus adult peripheral blood.** *J Immunol* 2004, **172**:5870-5879.
- Hirschfeld M, Ma Y, Weis JH, Vogel SN, Weis JJ: **Cutting edge: repurification of lipopolysaccharide eliminates signaling through both human and murine toll-like receptor 2.** *J Immunol* 2000, **165**:618-622.
- Bustin SA: **Quantification of mRNA using real-time reverse transcription PCR (RT-PCR): trends and problems.** *J Endocrinol* 2002, **29**:23-39.
- Tricarico C, Pinzani P, Bianchi S, Paglierani M, Distante V, Pazzaglia M, Busin SA, Orlando C: **Quantitative real-time reverse transcription polymerase chain reaction: normalisation to rRNA or single housekeeping genes is inappropriate for human tissue biopsies.** *Analytical Biochem* 2002, **309**:293-300.
- Knowlton N, Dozmorov IM, Centola M: **Microarray Data Analysis Toolbox (MDAT): for normalization, adjustment and analysis of gene expression data.** *Bioinformatics* 2004, **20**:3687-3690.
- Efron B, Gong G: **A leisurely look at the bootstrap, the jackknife, and cross-validation.** *American Statistician* 1983, **37**:36-48.
- Dozmorov I, Knowlton N, Tang Y, Shields A, Pathipvanich P, Jarvis JN, Centola M: **Hypervariable genes – experimental error or hidden dynamics.** *Nucleic Acids Res* 2004, **32**:e147.
- Johnson R, Wichern D: **Applied Multivariate Statistics.** Prentice Hall; 2002.
- Peters AM, Bertram P, Gahr M, Speer CP: **Reduced secretion of interleukin-1 and tumor necrosis factor-alpha by neonatal monocytes.** *Biol Neonate* 1993, **63**:157-62.
- Marwitz PA, Tenbergen-Meekes AJ, Heijnen CJ, Rijkers GT, Zegers BJ: **Interleukin 1 in the in vitro antigen-induced antibody response in the human adult and newborn.** *Scand J Immunol* 1990, **32**:451-459.
- Vanden Eijnden S, Goriely S, De Wit D, Goldman M, Willems F: **Preferential production of the IL-12(p40)/IL-23(p19) heterodimer by dendritic cells from human newborns.** *Eur J Immunol* 2006, **36**:21-26.
- Sullivan SE, Staba SL, Gersting JA, Hutson AD, Theriaque D, Christensen RD, Calhoun DA: **Circulating concentrations of chemok-**

- ines in cord blood, neonates, and adults. *Pediatr Res* 2002, **51**:653-657.
26. Juliano RL: **Signal transduction by cell adhesion receptors and the cytoskeleton: functions of integrins, cadherins, selectins, and immunoglobulin-superfamily members.** *Annu Rev Pharmacol Toxicol* 2002, **42**:283-323.
27. Swetman CA, Leverrier Y, Garg R, Gan CH, Ridley AJ, Katz DR, Chain BM: **Extension, retraction and contraction in the formation of a dendritic cell dendrite: distinct roles for Rho GTPases.** *Eur J Immunol* 2002, **32**:2074-2083.
28. Gillan L, Matei D, Fishman DA, Gerbin CS, Karlan BY, Chang DD: **Periostin secreted by epithelial ovarian carcinoma is a ligand for alpha(V)beta(3) and alpha(V)beta(5) integrins and promotes cell motility.** *Cancer Res* 2002, **62**:5358-5364.
29. Hamilton BJ, Burns CM, Nichols RC, Rigby WF: **Modulation of AUUUA response element binding by heterogeneous nuclear ribonucleoprotein A1 in human T lymphocytes. The roles of cytoplasmic location, transcription, and phosphorylation.** *J Biol Chem* 1997, **272**:28732-28741.
30. Morand EF, Bucala R, Leech M: **Macrophage inhibitory factor.** *Arthritis Rheum* 2003, **48**:291-299.
31. Roger T, Glauser MP, Calandra T: **Macrophage migration inhibitory factor (MIF) modulates innate immune responses induced by endotoxin and gram-negative bacteria.** *J Endotoxin Res* 2001, **7**:456-460.

Publish with **BioMed Central** and every scientist can read your work free of charge

"BioMed Central will be the most significant development for disseminating the results of biomedical research in our lifetime."

Sir Paul Nurse, Cancer Research UK

Your research papers will be:

- available free of charge to the entire biomedical community
- peer reviewed and published immediately upon acceptance
- cited in PubMed and archived on PubMed Central
- yours — you keep the copyright

Submit your manuscript here:  
[http://www.biomedcentral.com/info/publishing\\_adv.asp](http://www.biomedcentral.com/info/publishing_adv.asp)

